Effects of Modified Vermiculite on Water Absorbency and Swelling Behavior of Chitosan-*g*-Poly(Acrylic Acid)/Vermiculite Superabsorbent Composite

YUNTAO XIE[1,2] AND AIQIN WANG[1,*]

[1]*Center of Eco-material and Green Chemistry, Lanzhou Institute of Chemical Physics Chinese Academy of Sciences, Lanzhou, 730000, P.R. China*

[2]*Graduate University of the Chinese Academy of Sciences, Beijing, 100049, P.R. China*

ABSTRACT: In this study, a series of chitosan-*g*-poly(acrylic acid)/vermiculite (CTS-*g*-PAA/VMT) superabsorbent composites containing VMT, acid-activated, ion-exchanged, and organic modified VMT were synthesized by free-radical graft polymerization in aqueous solution, using *N,N*'-methylenebisacrylamide as a cross-linker and ammonium persulfate as an initiator. The effects of VMT and modified VMT on equilibrium water absorbency, swelling rate, and swelling behavior in various cationic saline solutions (NaCl, $CaCl_2$, and $FeCl_3$) and different pH value solution of superabsorbent composites were systematically investigated. FTIR spectroscopy confirmed that acrylic acid had been grafted onto CTS and the –OH groups of VMT participated reaction. The introduction of acid-activated, ion-exchanged, and organic modified VMT into chitosan-*g*-poly(acrylic acid) polymeric network could improve water absorbency and swelling rate compared with that of VMT. The water-absorbing capacity of superabsorbent composites decrease gradually with the increasing of the concentration of NaCl, $CaCl_2$, and $FeCl_3$ solutions from 0.01 to 10 mM. The all prepared samples have similar swelling behavior in different pH value solution and the equilibrium water absorbencies of samples keep roughly constant in the pH range from 4 to 12.

KEY WORDS: chitosan, modified vermiculite, superabsorbent composite, swelling.

INTRODUCTION

A SUPERABSORBENT IS A new kind of functional polymer that has a weakly crosslinked 3D network structure and the ability to absorb, swell, and retain aqueous fluids up to hundreds of times their own weight, and the water is hardly removed even under some pressure [1]. Owing to their excellent properties, superabsorbents have received

*Author to whom correspondence should be addressed. E-mail: aqwang@lzb.ac.cn

0021-9983/09/00 0001–17 $10.00/0 DOI: 10.1177/0021998309344644

considerable research and have been used in many fields such as healthcare products, agriculture and horticulture, wastewater treatment, medicine for drug-delivery systems, and other numerous applications [2,3]. With further development of superabsorbents, material researchers have realized that the swelling ability, gel strength, and thermal stability of superabsorbents can be altered by using some inorganic particles as additives. Many types of inorganic clay, such as kaolin [4], mica [5], attapulgite [6], vermiculite [7], bentonite [8], sepiolite [9], diatomite [10], and rectorite [11] have been introduced into poly(acrylic acid) and polyacrylamide polymeric network to form organic–inorganic composite. However, the structure and physicochemical properties of clay have played an important role in the performance of corresponding superabsorbent composite. The constituent and internal physicochemical environment of clay could be changed and improved through treating with acid- and heat-activated, ion-exchanged and organified treatment, as well as influence properties of corresponding superabsorbent composites [12–14].

Vermiculite (VMT) belongs to the general family of 2:1 layered silicates. This clay contains either Al^{3+} or Mg^{2+} and Fe^{3+} as normal octahedral ions, and a tetrahedral sheet in which Al^{3+} occurs as a substituted ion in place of some of the Si^{4+} [15]. Compared to other clay, VMT is abundant and has a larger cation exchange capacity (CEC), where the change of its physicochemical properties take place by ion exchange reaction [16]. Furthermore, there are reactive –OH groups on the surface of VMT and these groups are accessible to prepare organic–inorganic superabsorbent composites [17].

Recently, because of their availability, nontoxic characterization, biodegradability as well as biocompatibility, superabsorbents prepared through chemical modification of natural polymers such as starch [18], chitin and its derivatives chitosan [19], alginate [20], pectin [21], and guar gum [22] have attracted extensively investigated. Chitosan (CTS), the most abundant natural amino polysaccharide with specific structure and properties, has abundant hydroxyl and highly reactive amino groups distributed on its chains, which allow it to be easily modified through various chemical modifications. Grafted copolymerization of hydrophilic vinyl monomers onto CTS is considered to be an efficient approach to prepare superabsorbents [23].

Based on our recent work about modified attapulgite [24], montmorillonite [13] and sepiolite [14] doped with poly(acrylic acid) superabsorbent composites, in this work, a series of modified VMT were incorporated into the chitosan-*g*-poly (acrylic acid) (CTS-*g*-PAA) polymeric network and the effects of VMT, acid-activated, ion-exchanged and organic modified VMT on equilibrium water absorbency, swelling rate, swelling behavior in various cationic saline solutions (NaCl, $CaCl_2$, and $FeCl_3$), and different pH value solution of superabsorbent composites were systematically investigated. This work may be helpful in understanding the role of clay's modification in superabsorbent composite.

MATERIALS AND METHODS

Materials

Acrylic acid (AA, chemically pure, distilled under reduced pressure before use), ammonium persulfate (APS, analytical grade, recrystallized from distilled water before use), and *N,N*'-methylenebisacrylamide (MBA, chemically pure used as received) were supplied by Shanghai Reagent Corp. (Shanghai, China). Hexadecyltrimethyl ammonium bromide

(HDTMABr) was supplied by Beijing Chemical Reagents Company (Beijing, China). Chitosan (CTS, degree of deacetylation is 0.90, average molecular mass is 300 kDa) was supplied by Zhejiang Yuhuan Ocean Biology Co., China. Vermiculite (VMT, Xinyi Science and Technology Co., Ltd, Linze, Gansu, China) was milled through a 320-mesh screen. Other agents used were all of analytical grade and all solutions were prepared with distilled water.

Acid-Activation, Ion-exchanged, and Organic Modification of VMT

Acid-activated VMT (AVMT) samples were obtained according to the following method. 10.0 g VMT micro-powder was immersed in 100 mL HCl solution of various concentrations (2, 4, 6, 8, and 12 mol/L) at room temperature for 2.0 h at 1250 rpm stirring. The AVMT samples were washed with distilled water until pH = 6 was achieved, and then dried at 105°C for 8 h and milled and passed through a 320-mesh screen prior to use.

Ion-exchanged VMT (IVMT) samples were obtained according to the following method. Ten grams of VMT powder was added to 100 mL of salt solution containing 1 mol/L of either KCl, NaCl, $MgCl_2$, $CaCl_2$, $AlCl_3$, $FeCl_3$, K_2SO_4, K_3PO_4, K_2HPO_4, or KH_2PO_4 at room temperature for 1.0 h at 1250 rpm stirring. The ion-exchanged samples were washed with distilled water until the precipitation cannot be detected by 0.1 mol/L $AgNO_3$ aqueous solution in the filtrate, and then dried at 105°C for 8 h and milled and passed through a 320-mesh screen prior to use.

Organic modified VMT (OVMT) with different organification degree was synthesized as follows: different amounts of HDTMABr were dissolved in 100 mL distilled water in 250 mL flask, and then 10.0 g VMT was added into the flask. The mixture was stirred vigorously for 2 h at room temperature. Then the product was washed and filtrated repeatedly until no Br^- was detected by 0.1 mol/L $AgNO_3$ aqueous solution in the filtrate. The product was dried for several hours to constant weight at 105°C on an oven and then milled to 320-mesh size for further use.

Measurement of Organification Degree of OVMT

The organification degree of OVMT denotes the weight percent of organic cation of HDTMABr in the OVMT and it was measured as follows: 1.0 g OVMT with different organification degree and VMT were accurately weighted to the crucible respectively and then put into muffle. The muffle was heated to 800°C for several hours until those samples were calcined to constant weight. After transferring into desiccator and cooling to room temperature, those samples were weighed and organification degree of OVMT was calculated according to the following equations:

$$\mathrm{OD} = h - p \tag{1}$$

$$h, p = [(m_1 - m_2)/m_1] \times 100 \tag{2}$$

where OD is organification degree of OVMT, h and p are the weight loss ratio of OVMT and VMT, respectively, m_1 and m_2 are the weight of the samples before and after calcining, respectively.

Preparation of CTS-*g*-PAA/(VMT, AVMT, IVMT, and OVMT) Superabsorbent Composites

CTS-*g*-PAA/(VMT, AVMT, IVMT, and OVMT) superabsorbent composites were synthesized according to the following procedure. Appropriate amount of CTS was dissolved in 30 mL acetic acid solution (1% v/v) in a 250 mL four-neck flask, equipped with a mechanical stirrer, a reflux condenser, a funnel, and a nitrogen line. After being purged with nitrogen for 30 min to remove the oxygen dissolved in the system, 0.0954 g APS was introduced to initiate CTS to generate radicals. Ten minutes later, the mixed solution of 3.60 g AA, 0.1198 g MBA, appropriate amount VMT (AVMT, IVMT, and OVMT), and 10 mL water were added. The water bath was kept at 80°C for 3 h to complete the polymerization. The resulting product was washed with distilled water to remove residual reactant and transferred into sodium hydroxide aqueous solution (2 mol/L) to be neutralized to pH = 7 and swollen to equilibrium in distilled water, and then dehydrated with methanol. The samples were spread on a dish to dry to a constant weight at 70°C in an oven after filtration. The product was milled and all samples used for test had a particle size in the range of 40–80 mesh. The CTS-*g*-PAA superabsorbent was similar to that of preparation of the CTS-*g*-PAA/VMT superabsorbent composite; clay was omitted.

Measurement of Water Absorbency and Swelling Behavior

0.05 g of superabsorbent composite was immersed in excess distilled water (500 mL) at an ambient temperature for 4 h to reach the swelling equilibrium. The swollen sample was then separated from unabsorbed water by filtering through a 100-mesh screen. Water absorbency of the superabsorbent composite, Q_{eq}, is calculated using the following equation:

$$Q_{eq} = (m_2 - m_1)/m_1 \tag{3}$$

Here m_1 and m_2 are the weights of the dry sample and the swollen sample, respectively and Q_{eq} is calculated as grams of water per gram of sample.

The swelling rate (Q_t) of the samples was measured according to the following process. 0.05 g of sample was immersed in certain amount of distilled water in several 500 mL beakers. At certain time intervals, the water absorbency of the sample was measured. The measurement condition is the same as that for equilibrium water absorbency.

The determination of water absorbency at various pH solutions was similar to that of above measurement. And pH values of the external solution were adjusted *via* addition of 0.1 mol/L HCl and 0.1 mol/L NaOH solutions. The effects of various pH solutions on water absorbency can then be determined. All samples were carried out three times repeatedly and the average values are reported in this article.

Characterizations

The FTIR spectra were recorded on a Nicolet NEXUS FTIR spectrometer in 4000–400 cm^{-1} region using KBr pellets. SEM studies were carried out in a JSM-5600LV SEM instrument (JEOL, Ltd) after coating the sample with gold film using an acceleration voltage of 20 kV.

RESULTS AND DISCUSSION

Infrared Spectra Analysis

The infrared spectra of VMT and modified VMT are depicted in Figure 1. The main characteristic bands of VMT at 3670 cm^{-1} and 3427 cm^{-1}, 1622 cm^{-1}, 998 cm^{-1}, 686 cm^{-1} and 456 cm^{-1} are ascribed to –OH stretching, bending of –OH, Si–O asymmetric stretching, Si–O–Si symmetric stretching, and bending of Si–O (Figure 1(a)), respectively [25,26]. These adsorption peaks undergo some changes after modified with acid-activated, ion-exchanged, and organic modified treatment (Figure 1(b)–(e)); it is indicated that the exchange reaction between ions on the surface and channel of VMT with H^+, metal ions, and HDTMABr in external solutions has been carried out. Compared with the spectrum of VMT, the adsorption peak of AVMT at 1422 and 878 cm^{-1}, which are ascribed to CO_3^{2-} stretching vibration disappeared in Figure 1(b); these changes indicated carbonates were removed from VMT after acid-activated treatment. And the new adsorption peak of OVMT at 2920, 2851, and 1472 cm^{-1}, which are ascribed to asymmetric and symmetric stretching vibration of C–H bonds and C–N bending vibration of alkylammonium chain appeared (Figure 1(e)), indicating organic cations of HDTMABr have been exchanged with VMT [15].

IR spectra of CTS-*g*-PAA, CTS-*g*-PAA/VMT, CTS-*g*-PAA/AVMT, CTS-*g*-PAA/IVMT, and CTS-*g*-PAA/OVMT are shown in Figure 2. It can be seen from IR spectra of CTS-*g*-PAA that the characteristic bands at 1567 cm^{-1} (–COOH stretching vibration), 1453 cm^{-1} (asymmetric stretching vibration), and 1408 cm^{-1} (symmetric stretching vibration of $–COO^-$) appeared (Figure 2(a)). The absorption peak at 1325 cm^{-1} (stretching and bending vibrations of the C–N bond of the amide III of CTS) also appeared. However, the

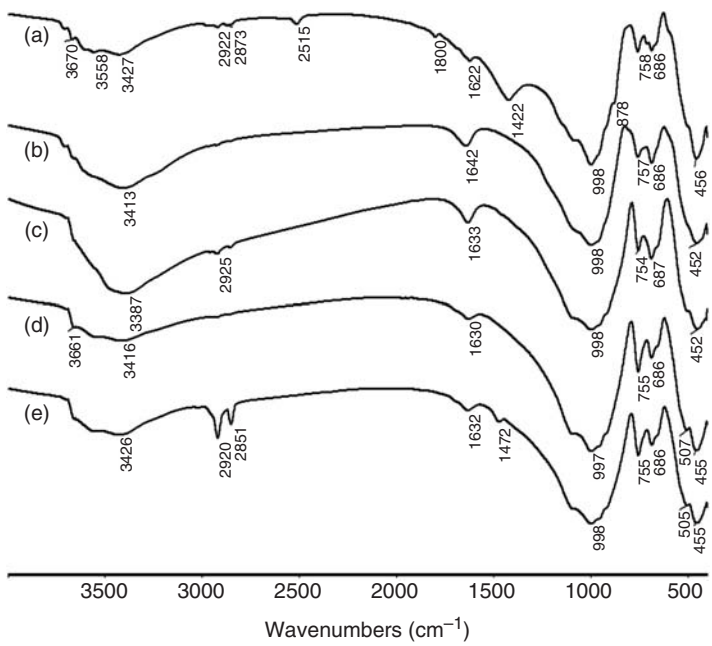

Figure 1. *IR spectra of: (a) VMT, (b) AVMT, (C) Fe^{3+}-VMT, (d) KH_2PO_4-VMT, and (e) OVMT.*

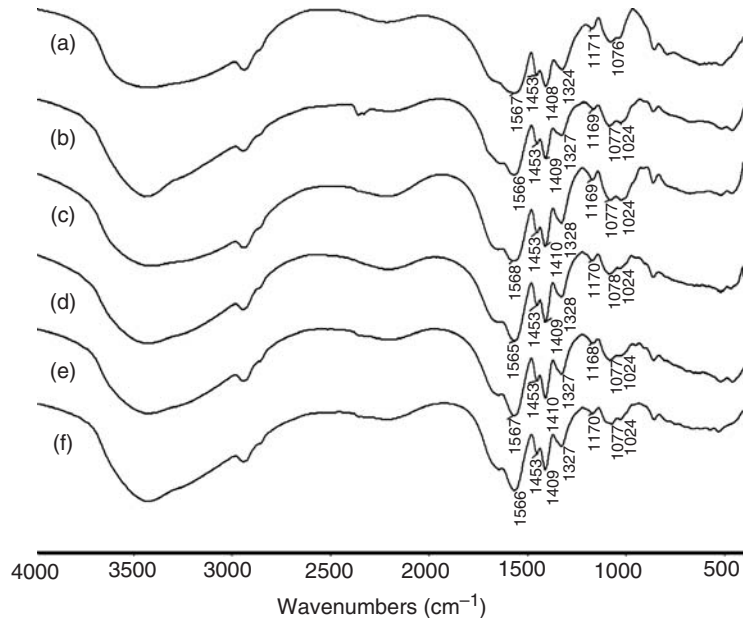

Figure 2. *IR spectra of: (a) CTS-g-PAA, (b) CTS-g-PAA/VMT, (c) CTS-g-PAA/AVMT, (d) CTS-g-PAA/Fe^{3+}-VMT, (e) CTS-g-PAA/KH_2PO_4-VMT, and (f) CTS-g-PAA/OVMT, respectively. Clay content in the feed is 10 wt%.*

characteristic absorption peaks of the amide I (1660 cm^{-1}), N–H (1598 cm^{-1}), and C_6–OH (1094 cm^{-1}) of CTS could not be found, whose information confirms that $-NH_2$, –NHCO, and –OH of CTS took part in graft reaction with AA [27]. When the composites are formed, the characteristic peaks of VMT at 3670 and 1622 cm^{-1} are ascribed to the stretching vibration and bending vibration of –OH on the surface of layers of VMT, which disappeared in the spectrum of these composites. The absorption band at 998 cm^{-1} (assigned to Si–O stretching vibration) of VMT and modified VMT disappear and the new absorption band at 1024 cm^{-1} appear in the spectrum of these composites and this peak weakened obviously after polymerization reaction (Figure 2(b)–(f)). On the whole, the above analysis results indicate that VMT and modified VMT also participated in the grafting copolymerization reaction through its active Si–OH groups.

Effect of AVMT on Water Absorbency

Figure 3 displays the effect of HCl concentration while acidifying VMT on CTS-*g*-PAA/AVMT superabsorbent composite. It can be seen from Figure 3, the water absorbency in distilled water of CTS-*g*-PAA/AVMT composites increases from 279.5 to 312.8 $g\,g^{-1}$ with HCl concentration increasing from 2 to 6 mol/L, and then decreasing to 301.4 $g\,g^{-1}$ with HCl concentration further increasing to 12 mol/L. The water absorbency in 0.9 wt% NaCl solution is in the range of 48.2–60.4 $g\,g^{-1}$. Compared with the water absorbency of CTS-*g*-PAA/VMT (223.3 $g\,g^{-1}$, 51.0 $g\,g^{-1}$), the water absorbency of CTS-*g*-PAA/AVMT composites activated with 6 mol/L HCl solution is superior to that of the other sample, and the water absorbency is 312.8 and 57.5 $g\,g^{-1}$ in distilled water and 0.9 wt% NaCl solution, respectively. From the results of IR analysis, we can conclude that carbonate exists in VMT. Treatment with HCl removes carbonate and more Si–OH of VMT appears to

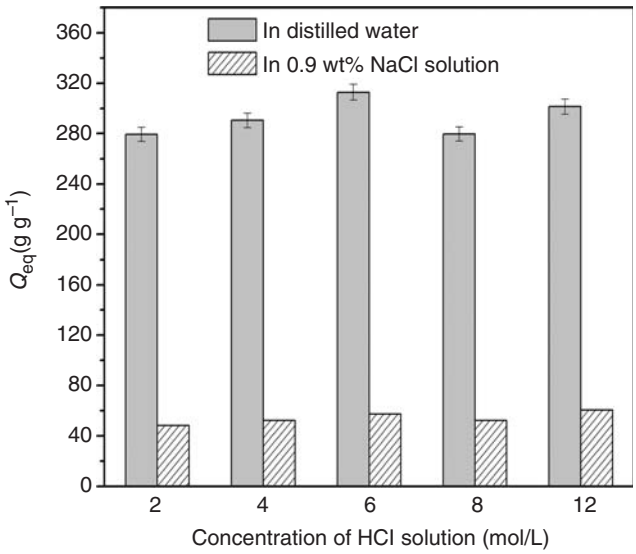

Figure 3. *Variation of water absorbency for the CTS-g-PAA/AVMT superabsorbent composites with HCl solution concentration while acidifying VMT. AVMT content in the feed is 10 wt%.*

participate in the polymerization reaction, which forms a more regular polymeric network structure and endows the CTS-*g*-PAA/VMT composite with higher water absorbency. However, when HCl concentration increases beyond 6 mol/L, more cations on the surface of VMT are exchanged by H^+, and then the amount of active cation site decreases evidently, which goes against the formation of polymeric network, and then results in the decrease of water absorbency [28]. Therefore, the variation of water absorbency with HCl concentration indicates that a moderate HCl concentration is needed to enhance water absorbency of the composite.

Effect of IVMT on Water Absorbency

There are many interior channels in the structure of VMT, which allows entrance of organic and inorganic ions. Thus, cations and anions in the solution could exchange with them through ion-exchanged process and then alter the constituent of VMT. This characteristic is similar to that of sepiolite [14]. Effects of the cation-exchanged and anion-exchanged VMT on water absorbency of CTS-*g*-PAA/VMT superabsorbent composite in distilled water and 0.9 wt% NaCl solution are shown in Figure 4, respectively. It can be seen from Figure 4, to the series of cation-exchanged VMT, the water absorbency in distilled water increases in the order VMT < Mg^{2+}-VMT < Al^{3+}-VMT < Li^+-VMT < Ca^{2+}-VMT < Na^+-VMT < K^+-VMT < AVMT < Fe^{3+}-VMT, the highest water absorbency of Fe^{3+}-VMT reaches to 326.2 g g^{-1}. And to the series of anion-exchanged VMT, the water absorbency increases in the order VMT < SO_4^{2-}-VMT < $H_2PO_4^{2-}$-VMT < PO_4^{3-}-VMT < Cl^--VMT < AVMT < $H_2PO_4^-$-VMT, the highest water absorbency of $H_2PO_4^-$-VMT is 324.8 g g^{-1}. The most of the water absorbency in 0.9 wt% NaCl solution of all samples is in the range of 50–60 g g^{-1}. The water absorbency of all samples improved obviously with introducing ion-exchanged VMT compared with that of VMT.

This result can be explained as follows: on one hand, VMT may contain some soluble salts and impurities which could be removed after ion-exchanged process and then ion exchange enhanced the hydrophilicity of the composite and made it swell even more. On the other hand, the ionization of acid phosphate helps to get rid of the carbonate of VMT and this process is similar to acidification. Furthermore, some divalent and trivalent cations may form intermolecular and intramolecular complex with hydrophilic groups (such as $-COO^-$, –COOH, and –OH) of the polymerization system, and help MBA to form a more regular polymeric network, which improves the water absorbency of the corresponding superabsorbent composite.

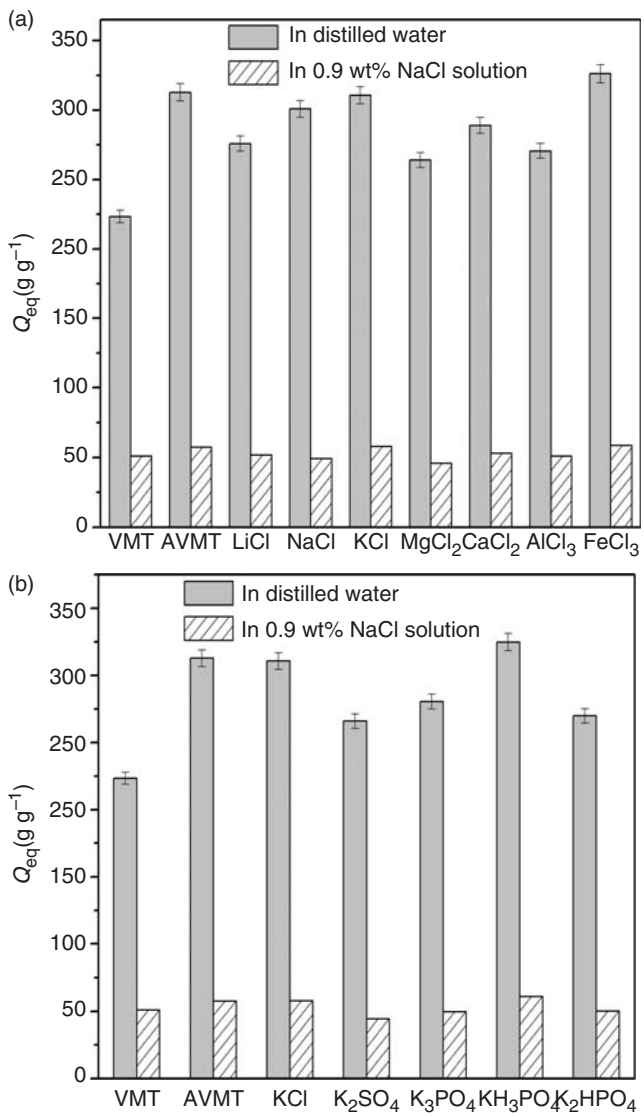

Figure 4. *Effect of cations and anions on water absorbency of the superabsorbent composites in distilled water and 0.9 wt% NaCl solution. Clay content in the feed is 10 wt%.*

Effect of OVMT on Water Absorbency

Water absorbency of CTS-*g*-PAA/VMT and CTS-*g*-PAA/OVMT series superabsorbent composites in distilled water and in 0.9 wt% NaCl solution were measured and are shown in Figure 5. We can see from Figure 5 that the water absorbency for the CTS-*g*-PAA/OVMT with different organification degree series are always higher than that of the CTS-*g*-PAA/VMT in distilled water and in the range of 313.5–333.2 g g^{-1}. When the organification degree of OVMT is 2.06%, the water absorbency both in distilled water and in 0.9 wt% NaCl solution reaches to the maximum. This is attributed to the fact that the introduction of OVMT into CTS-*g*-PAA polymeric network improved the polymeric network to a higher extent, comparing with that of the doped with VMT. One part of long alkyl chains of HDTMABr attached onto the surface of VMT microparticles and the other entered into the interlayer of VMT, which improve the polymeric network by forming tiny hydrophobic regions, and also weakened the hydrogen bonding interaction among hydrophilic groups [29].

In order to further illuminate the function of VMT and modified VMT to the polymeric network of composites, the SEM images of CTS-*g*-PAA and a series of CTS-*g*-PAA/VMT superabsorbent composites are displayed in Figure 6. As can be seen from the Figure 6, the surface morphology of CTS-*g*-PAA is dissimilar with the series of CTS-*g*-PAA/VMT. CTS-*g*-PAA (Figure 6(a)) shows a compact and folded surface whose structure goes against the fast permeation of water into the polymeric network. On introducing VMT to the CTS-*g*-PAA (Figure 6(b)), the surface morphology of CTS-*g*-PAA/VMT appears to be spongy, loose and in an unorganized state, and this structure will be helpful for the improvement of swelling rate. Compared with that of CTS-*g*-PAA/VMT, the surface morphology of CTS-*g*-PAA/AVMT (Figure 6(c)), CTS-*g*-PAA/Fe^{3+}-VMT (Figure 6(d)), CTS-*g*-PAA/KH_2PO_4-VMT (Figure 6(e)), and CTS-*g*-PAA/OVMT (Figure 6(f)) present more regular and organized states besides having analogous porous structure, which results from these SEM images being consistent with the statement above mentioned.

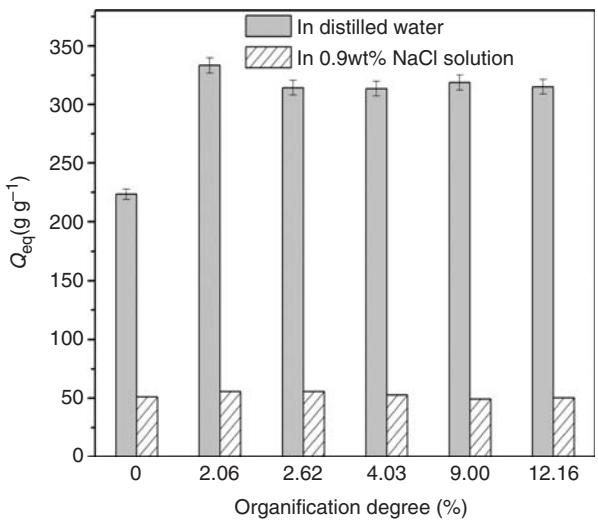

Figure 5. *Variation of water absorbency for the superabsorbent composites in distilled water with different organification degree.*

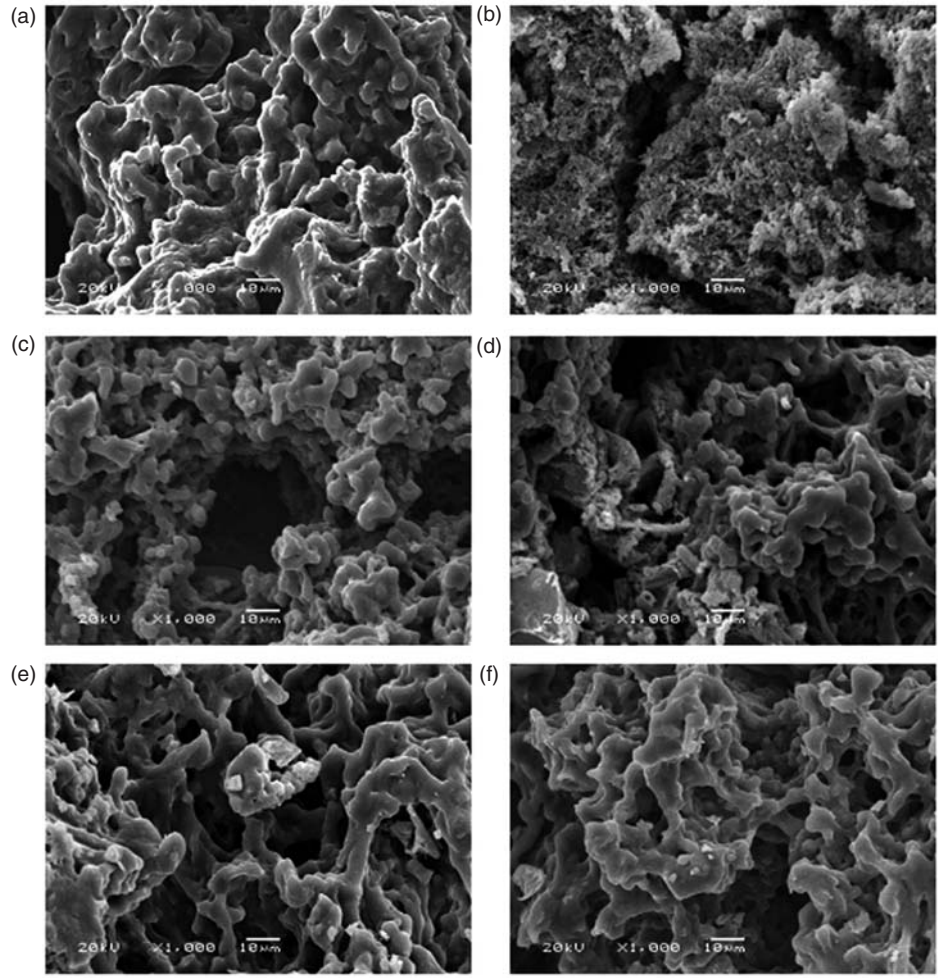

Figure 6. *SEM micrographs of: (a) CTS-g-PAA, (b) CTS-g-PAA/VMT, (c) CTS-g-PAA/AVMT, (d) CTS-g-PAA/Fe^{3+}-VMT, (e) CTS-g-PAA/KH_2PO_4-VMT, and (f) CTS-g-PAA/OVMT, respectively. Clay content in the feed is 10 wt%.*

Effect of the Content of Different Treatment VMT on Water Absorbency

The influence of the content of different treatment VMT on water absorbency in distilled water of superabsorbent composites is exhibited in Figure 7. It is obvious that the trend of VMT and treated VMT samples on water absorbency with increasing clay content is different. The water absorbency of CTS-*g*-PAA/VMT decreases with increasing the clay content from 0 to 30 wt%, but that of CTS-*g*-PAA/AVMT, CTS-*g*-PAA/Fe^{3+}-VMT, CTS-*g*-PAA/KH_2PO_4-VMT, and CTS-*g*-PAA/OVMT increase with increasing the clay content from 0 to 5 wt% and decrease with further increasing the clay content. It is noticeable that the introduction of modified VMT into the composites could enhance the water absorbency compared with the falling of water absorbency with VMT introduction, and the water absorbency of the composites containing modified VMT is close to that of CTS-*g*-PAA when the VMT content reaches 30 wt%, which results in further elucidation of the function

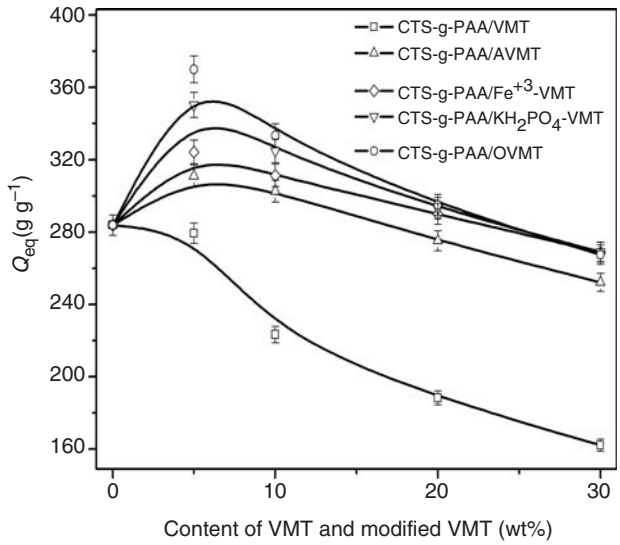

Figure 7. *Variation of water absorbency for the superabsorbent composites in distilled water with different treatment clay content.*

and significance of modified clay to its corresponding superabsorbent composites. This phenomenon is in conformity with our previous study on water absorbency of CTS-*g*-PAA/ST composites based on acidified sepiolite and cation-exchanged sepiolite [14].

Effect of Modified VMT on Swelling Behaviors in Saline Solutions

It is more important to know the behavior of a superabsorbent composite when it contacts with various saline solutions considering its practical applications. The swelling behaviors of modified VMT composites in three cationic saline solutions (NaCl, $CaCl_2$, and $FeCl_3$) were investigated, as shown in Figure 8(a)–(c). It can be seen from the Figure 8(a)–(c), the introduction of modified VMT to CTS-*g*-PAA could improve the salt-resistant ability in the three saline solutions, and the order of the salt-resistant ability of all testing samples is consistent with that of water absorbency in distilled water. And the absorbency of all testing samples is almost equal to that of in distilled water at lower saline concentration (0.01 mM for each saline solution); however, with an increase in ionic strength of external solution from 0.01 to 0.1 mM, a sluggish decrease in these swelling curves can be observed. On further increasing the concentration of external solution from 0.5 to 10 mM, the absorbency of all testing samples declined sharply. This phenomenon can be explained by the fact that at low ionic strength, the repulsion is a long-range interaction, and the gel expands to minimize the repulsion free energy [30]. When the ionic strength rises, the expansion of the network decreases because of screening effect of the ionic charges bound to the polymeric network and the decrease of osmotic pressure difference between the gel and the external solution. This is a typical polyelectrolyte behavior [31]. Additionally, we can also see from Figure 8(a)–(c), the swelling capability of all samples in NaCl solution is higher than those of in $CaCl_2$ and $FeCl_3$ solution. This is because that multivalent Ca^{2+} and Fe^{3+} ions may coordinate with the carboxylate groups on adjacent chains or chain segments of the copolymer, which lead to the increasing of

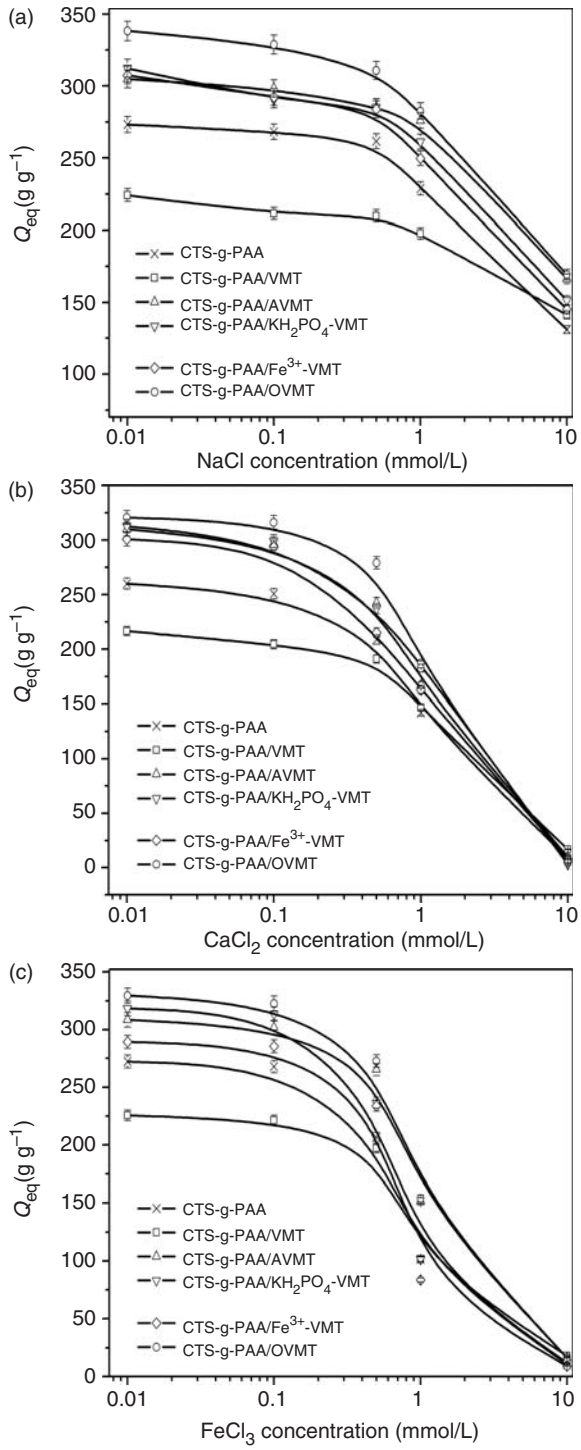

Figure 8. *Equilibrium water absorbency of the superabsorbent composites in NaCl, $CaCl_2$ and $FeCl_3$ solutions with various concentrations.*

crosslink density and then the polymeric network is sharply shrinkable thereupon too. These results are similar to our recent work about poly(acrylic acid-co-acrylamide)/montmorillonite/sodium humate superabsorbent composites [13].

Effect of Various pH Solutions on Water Absorbency

Figure 9 displays the effect of various pH solutions on water absorbency. As can be seen from Figure 9, the water absorbency of all testing samples sharply increases at the pH range from 2 to 4 and decreases at the pH range from 10 to 13, but almost keeps constant at pH 4–10. This is because these superabsorbent composites are anionic-type superabsorbent polymers, which contain a majority of hydrophilic –COOH and $-COO^-$ groups, and which play an important role in swelling behavior and result in water absorbency changes through different interaction species in various pH solutions. $-COO^-$ groups can combine with H^+ of the external solution under an acidic condition, and –COOH groups can react with external OH^- to convert to $-COO^-$ under a basic condition. As a result, the amount of H^+ and OH^- in the external solution may decrease in the pH range of 4–11 because of the buffer action of –COOH and $-COO^-$ groups [32]. When the pH of external solution increases from 2 to 4, the ionized degree of these hydrophilic groups increase, which result in an increase in osmotic pressure between polymeric network and external solution as well as electrostatic repulsion among carboxylate groups inside the polymer matrix [33]. Consequently, the network spaces of the composites more easily expand and hold more liquid. However, when the pH is beyond 10, the increased ionic strength of the swelling medium causes the sharp reducing of osmotic pressure and ultimately decreases the equilibrium water absorbency of the superabsorbent composites. This phenomenon is in conformity with our previous study [13,14]. Remarkably, the water absorbency of the superabsorbent composites at a wide range of pH from 4 to 10 is very close and almost equal to its equilibrium water absorbency in distilled water, which is the characteristic of

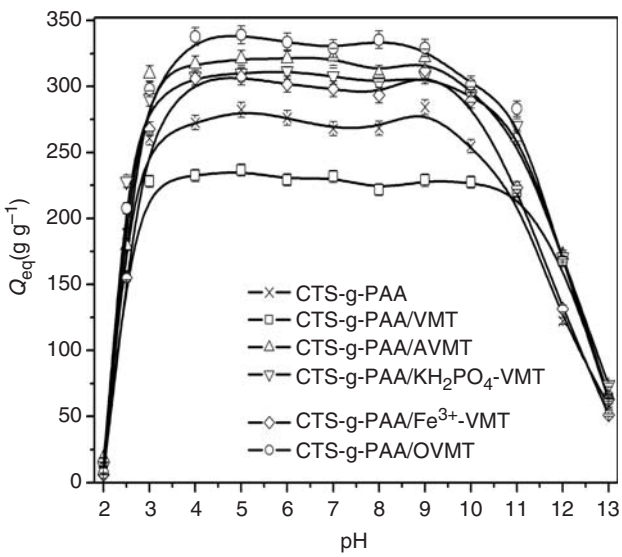

Figure 9. *Effect of pH of external solution on water absorbency.*

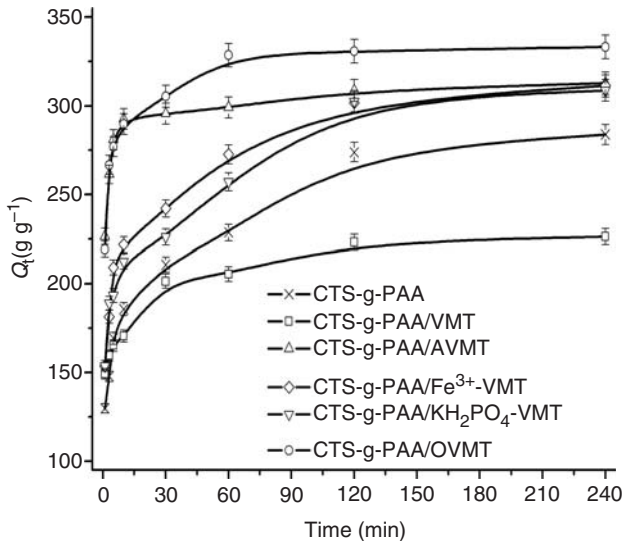

Figure 10. *Swelling rate of superabsorbent composites in distilled water.*

poly(acrylic acid)-based superabsorbent. This characteristic is helpful in the application of superabsorbent composites in agriculture and horticulture.

Swelling Rate and Swelling Dynamics of Superabsorbent Composites

Figure 10 shows the swelling rate of superabsorbent composites in distilled water. It is found that the swelling rate of all superabsorbent composites is higher in 0–10 min, and the time of reaching swelling equilibrium is about 2 h. The swelling kinetics was characterized by the Voigt-based viscoelastic model [34,35]:

$$S_t = p(1 - e^{-t/r}) \tag{4}$$

where S_t is the swelling capability at any moment (g g^{-1}), p is the power parameter (g g^{-1}), t is the time (min), and r is the rate parameter (time required to reach 0.63 of equilibrium swelling) (min). The rate parameter, r, is a measure of the swelling rate of a superabsorbent sample so that a lower r-value can reflect a quicker swelling rate. The power parameter, p, denotes the water-holding capacity of an individual superabsorbent.

The data obtained from the equilibrium swelling and the swelling rate for each sample was fitted into the above equation to find the values of the rate and power parameters which are displayed in Table 1. These parameters could reflect the quickness or slowness of all samples in certain degree. The swelling rate is in the order CTS-*g*-PAA/AVMT > CTS-*g*-PAA/VMT > CTS-*g*-PAA/OVMT > CTS-*g*-PAA/KH_2PO_4-VMT > CTS-*g*-PAA/Fe^{3+}-VMT > CTS-*g*-PAA.

From the results of fitting with Voigt-based viscoelastic model about swelling kinetics of these composites, it can be concluded that the incorporation of VMT and modified VMT into the composites could enhance the swelling rate. Moreover, introducing modified VMT could also improve water-holding capacity. This is because that the composites containing VMT and modified VMT have porous and loose structure, which can be

Table 1. The parameters of the Voigt-based viscoelastic swelling kinetics model of samples.

Samples	Parameters P (gg^{-1})	r (min)
CTS-g-PAA	236.73	2.85
CTS-g-PAA/VMT	194.61	0.77
CTS-g-PAA/AVMT	294.35	0.72
CTS-g-PAA/Fe^{3+}-VMT	265.61	2.10
CTS-g-PAA/KH_2PO_4-VMT	253.83	1.76
CTS-g-PAA/OVMT	307.32	0.88

confirmed by SEM in Figure 6, and the structure can contribute water molecules to penetrate quickly into the polymeric network from the external solution. The statement is conformity with our previous work [13].

CONCLUSIONS

In this work, a series of VMT and modified VMT were incorporated into CTS-*g*-PAA polymeric network and the effects of different modified VMT on swelling properties of CTS-*g*-PAA/VMT composites were investigated. The results showed that the properties of the composite including water absorbency and swelling behavior were strongly dependent on H^+ concentration and the kinds of cation exchanged. The incorporation of long alkyl chains of HDTMABr can change the circumstance of surface and interlayer of VMT, which make CTS-*g*-PAA polymeric network to be ameliorated to a higher extent and therefore swells more. The surface morphology of CTS-*g*-PAA/modified VMT presents more regular and organized comparing with that of CTS-*g*-PAA/VMT from the results of SEM analysis. The introduction of suitable amount of modified VMT to CTS-*g*-PAA could not only enhance composites' water absorbency but also improve the swelling rate, water-holding capacity, and salt-resistant ability. Based on this work, we can conclude the simple and feasible modification of VMT is also an effective approach to improve the performance of organic–inorganic superabsorbent composites.

ACKNOWLEDGMENTS

This work was financially supported by the Western Action Project of CAS (No. KGCX2-YW-501) and '863' Project of the Ministry of Science and Technology, P. R. China (No. 2006AA03Z0454).

REFERENCES

1. Buchholz, F.L. and Graham, A.T. (1998). *Modern Superabsorbent Polymer Technology*, Wiley-VCH, New York.
2. Zohuriaan-Mehr, M.J. and Kabiri, K. (2008). Superabsorbent Polymer Materials: A Review, *Iran. Polym. J.*, **17**: 451–477.

3. Mudiyanselage, T.K. and Neckers, D.C. (2008). Highly Absorbing Superabsorbent Polymer, *J. Polym. Sci. Part A: Polym. Chem.*, **46**: 1357–1364.
4. Wu, J.H., Wei, Y.L., Lin, J.M. and Lin, S.B. (2003). Preparation of a Starch-Graft-Acrylamide/Kaolinite Superabsorbent Composite and the Influence of the Hydrophilic Group on its Water Absorbency, *Polym. Int.*, **52**: 1909–1912.
5. Lin, J.M., Wu, J.H., Yang, Z.F. and Pu, M.L. (2001). Synthesis and Properties of Poly(Acrylic Acid)/Mica Superabsorbent Nanocomposite, *Macromol. Rapid. Commun.*, **22**: 422–424.
6. Li, A., Wang, A.Q. and Chen, J.M. (2004). Studies on Poly(Acrylic Acid)/Attapulgite Superabsorbent Composite. I. Synthesis and Characterization, *J. Appl. Polym. Sci.*, **92**: 1596–1603.
7. Zheng, Y.A., Li, P., Zhang, J.P. and Wang, A.Q. (2007). Study on Superabsorbent Composite XVI. Synthesis, Characterization and Swelling Behaviors of Poly (Sodium Acrylate)/Vermiculite Superabsorbent Composites, *Eur. Polym. J.*, **43**: 1691–1698.
8. Santiago, F., Mucientes, A.E., Osorio, M. and Rivera, C. (2007). Preparation of Composites and Nanocomposites Based on Bentonite and Poly (Sodium Acrylate). Effect of Amount of Bentonite on the Swelling Behaviour, *Eur. Polym. J.*, **43**: 1–9.
9. Zhang, F.Q., Guo, Z.J., Gao, H., Li, Y.C., Ren, L., Shi, L. and Wang, L.X. (2005). Synthesis and Properties of Sepiolite/Poly (Acrylic Acid-Coacrylamide) Nanocomposites, *Polym. Bull.*, **55**: 419–428.
10. Qi, X.H., Liu, M.Z., Chen, Z.B. and Liang, R. (2007). Preparation and Properties of Diatomite Composite Superabsorbent, *Polym. Adv. Technol.*, **18**: 184–193.
11. Liu, J.H. and Wang, A.Q. (2008). Study on Superabsorbent Composites XXI. Synthesis, Characterization and Swelling Behaviors of Chitosan-*g*-Poly(Acrylic Acid)/Organo-Rectorite Nanocomposite Superabsorbents, *J. Appl. Polym. Sci.*, **110**: 678–686.
12. Su, X.F., Zhang, G., Xu, K., Wang, J.H., Song, C.L. and Wang, P.X. (2008). The Effect of MMT/Modified MMT on the Structure and Performance of the Superabsorbent Composite, *Polym. Bull.*, **60**: 69–78.
13. Zheng, Y.A. and Wang, A.Q. (2009). Study on Superabsorbent Composite. XX. Effects of Cation-Exchanged Montmorillonite on Swelling Properties of Superabsorbent Composite Containing Sodium Humate, *Polym. Compos.*, **30**: 1138–1145.
14. Xie, Y.T., Wang, A.Q. and Liu, G. Superabsorbent Composite XXII: Effects of Modified Sepiolite on Water Absorbency and Swelling Behavior of Chitosan-*g*-Poly (Acrylic Acid)/Sepiolite Superabsorbent Composite, *Polym. Compos.*, DOI 10.1002/pc.20770.
15. Xu, J., Li, R.K.Y., Xu, Y., Li, L. and Meng, Y.Z. (2005). Preparation of Poly (Propylene Carbonate)/Organo-Vermiculite Nanocomposites via Direct Melt Intercalation, *Eur. Polym. J.*, **41**: 881–888.
16. Fonseca, M.G., Oliveira, M.M., Arakaki, L.N.H., Espinola, J.G.P. and Airoldi, C. (2005). Natural Vermiculite as an Exchanger Support for Heavy Cations in Aqueous Solution, *J. Colloid Interf. Sci.*, **285**: 50–55.
17. Xie, Y.T. and Wang, A.Q. (2009). Study on Superabsorbent Composites XIX. Synthesis, Characterization and Performance of Chitosan-*g*-Poly (Acrylic Acid)/Vermiculite Superabsorbent Composites, *J. Polym. Res.*, **16**: 143–150.
18. Lanthong, P., Nuisin, R. and KiatKamjornwong, S. (2006). Graft Copolymerization, Characterization, and Degradation of Cassava Starch-*g*-Acrylamide/Itaconic Acid Superabsorbents, *Carbohydr. Polym.*, **66**: 229–245.
19. Yoshimura, T., Uchikoshi, I., Yoshiura, Y. and Fujioka, R. (2005). Synthesis and Characterization of Novel Biodegradable Superabsorbent Hydrogels Based on Chitin and Succinic Anhydride, *Carbohydr. Polym.*, **61**: 322–326.
20. Marandi, G.B., Sharifnia, N. and Hosseinzadeh, H. (2006). Synthesis of an Alginate-Poly (Sodium Acrylate-Co-Acrylamide) Superabsorbent Hydrogel with Low Salt Sensitivity and High pH Sensitivity, *J. Appl. Polym. Sci.*, **101**: 2927–2937.
21. Yoshimura, T., Sengoku, K. and Fujioka, R. (2005). Pectin-based Surperabsorbent Hydrogels Crosslinked by Some Chemicals: Synthesis and Characterization, *Polym. Bull.*, **55**: 123–129.

22. Wang, W.B., Zheng, Y.A. and Wang, A.Q. (2008). Syntheses and Properties of the Superabsorbent Composites Based on Natural Guar Gum and Attapulgite, *Polym. Adv. Technol.*, **19**: 1852–1859.
23. Chen, Y. and Tan, H.M. (2006). Crosslinked Carboxymethylchitosan-*g*-Poly(Acrylic Acid) Copolymer as a Novel Superabsorbent Polymer, *Carbohydr. Res.*, **341**: 887–896.
24. Zhang, J.P., Chen, H. and Wang, A.Q. (2007). Study on Superabsorbent Composite. XV. Effects of Ion-exchanged Attapulgite on Water Absorbency of Superabsorbent Composites, *Polym. Compos.*, **28**: 208–213.
25. Tomanec, R., Popov, S., Vučinič, D. and Lazič, P. (1997). Vermiculite from Kopaonik (Yugoslavia) Characterization and Processing, *Physicochem. Prob. Miner. Process.*, **31**: 247–254.
26. Tang, Q.W., Lin, J.M., Wu, J.H., Xu, Y.W. and Zhang, C.J. (2007). Preparation and Water Absorbency of a Novel Poly (Acrylate-Co-Acrylamide)/Vermiculite Superabsorbent Composite, *J. Appl. Polym. Sci.*, **104**: 735–739.
27. Zhang, J.P., Wang, Q. and Wang, A.Q. (2007). Synthesis and Characterization of Chitosan-*g*-Poly(Acrylic Acid)/Attapulgite Superabsorbent Composites, *Carbohydr. Polym.*, **68**: 367–374.
28. Wang, W.J., Zhang, J.P., Chen, H. and Wang, A.Q. (2006). Study on Superabsorbent Composite. VIII. Effects of Acid- and Heat-activated Attapulgite on Water Absorbency of Polyacrylamide/Attapulgite, *J. Appl. Polym. Sci.*, **103**: 2419–2424.
29. Zhang, J.P., Chen, H. and Wang, A.Q. (2006). Study on Superabsorbent Composite. IV. Effects of Organification Degree of Attapulgite on Swelling Behaviors of Polyacrylamide/Organo-Attapulgite Composites, *Eur. Polym.*, **42**: 101–108.
30. Kiatkamjornwong, S., Mongkolsawat, K. and Sonsuk, M. (2002). Synthesis and Property Characterization of Cassava Starch Grafted Poly [Acrylamide-Co-(Maleic Acid)] Superabsorbent via γ-Irradiation, *Polymer*, **43**: 3915–3924.
31. Nisato, G., Munch, J.P. and Candau, S.J. (1999). Swelling, Structure, and Elasticity of Polyampholyte Hydrogels, *Langmuir*, **15**: 4236–4244.
32. Wang, W.B. and Wang, A.Q. (2009). Synthesis, Swelling Behaviors, and Slow-Release Characteristics of a Guar Gum-*g*-Poly (Sodium Acrylate)/Sodium Humate Superabsorbent, *J. Appl. Polym. Sci.*, **112**: 2102–2111.
33. Kiatkamjornwong, S., Chomsaksakul, W. and Sonsuk, M. (2000). Radiation Modification of Water Absorption of Cassava Starch by Acrylic Acid/Acrylamide, *Radiat. Phys. Chem.*, **59**: 413–427.
34. Omidian, H., Hashemi, S.A., Sammes, P.G. and Meldrum, I. (1998). A Model for the Swelling of Superabsorbent Polymers, *Polymer*, **39**: 6697–6704.
35. Kabiri, K., Omidian, H., Hashemi, S.A. and Zohuriaan-Mehr, M.J. (2003). Synthesis of Fast-Swelling Superabsorbent Hydrogels: Effect of Crosslinker Type and Concentration on Porosity and Absorption Rate, *Eur. Polym. J.*, **39**: 1341–1348.